# COMET GEOLOGY WITH DEEP IMPACT REMOTE SENSING

PETER C. THOMAS[1,*], JOSEPH VEVERKA[1], MICHAEL F. A'HEARN[2], LUCY MCFADDEN[2], MICHAEL J. S. BELTON[3] and JESSICA M. SUNSHINE[4]
[1] *Center for Radiophysics and Space Research, Cornell University, Ithaca NY, U.S.A.*
[2] *University of Maryland, College Park, MD, U.S.A.*
[3] *Belton Space Exploration Initiatives, LLC, Tucson, AZ, U.S.A.*
[4] *Science Applications International Corporation, Chantilly, VA, U.S.A.*
*(*Author for correspondence; e-mail: thomas@baritone.astro.cornell.edu)*

(Received 20 August 2004; Accepted in final form 3 December 2004)

**Abstract.** The Deep Impact mission will provide the highest resolution images yet of a comet nucleus. Our knowledge of the makeup and structure of cometary nuclei, and the processes shaping their surfaces, is extremely limited, thus use of the Deep Impact data to show the geological context of the cratering experiment is crucial. This article briefly discusses some of the geological issues of cometary nuclei.

**Keywords:** comets, geology, impacts, structure

## 1. Introduction

The long history of comet observations with telescopes contrasts dramatically with the very brief, recent period of close-up observations of comet nuclei from spacecraft. Fleeting views of comets Halley, Borrelly and Wild-2 have been obtained by flybys, but only the latter data have sufficient resolution to address geological questions concerning the morphology and surface processes of comet nuclei. Deep Impact seeks to explore actively a comet nucleus by impact excavation (A'Hearn *et al.*, this issue). The dynamic and compositional data obtained by observing the impact should provide new information about the properties of comet nuclei. An equally important goal is a detailed remote sensing survey of the nucleus that will put the impact in context, and provide by far the most detailed views of a comet to date. Here we review the investigation strategy and its application to questions concerning the nature and evolution of cometary nuclei. The global properties (including likely rotation state) of the nucleus of Tempel 1, inferred from accumulated telescopic data, are summarized by Belton *et al*. (this issue). The nucleus size, considerably elongated, with a mean radius of approximately 3.4 km, and a spin period of about 2 h, allows nearly half the surface to be imaged at a wide variety of viewing angles and in multiple colors. Here we focus on questions of surface process, morphology and related geological issues.

Space Science Reviews (2005) 117: 193–205
DOI: 10.1007/s11214-005-3391-7

## 2. Investigation Scheme

The cratering experiment is described by Schultz and Ernst (this issue). The flyby spacecraft, the impactor and the instruments are described by Hampton *et al*. (this issue). The flyby spacecraft carries two imagers, the High Resolution Imager (HRI) and a Medium Resolution Imager (MRI), each provided with a nine-position filter wheel. The respective fields of view and spatial resolution at 1000 km are 2 km, 2 m/pxl, and 10 km, 10 m/pixel. The impactor carries a copy of the MRI, the Impactor Targeting Sensor (ITS) but without color filters, for active targeting and high-resolution images of the impact site. The data taking scheme at encounter (Klaasen *et al*., this issue) allows for stereo imaging and rapid imaging of the nucleus and of the expanding plume and ejecta from the impact event, which occurs before closest approach of the flyby spacecraft. In addition, it provides for near-IR spectral mapping of the comet surface.

A day before impact, at a range of over 800000 km, the nucleus, about $14 \times 5 \times 5$ km (Belton *et al.*, this issue), is about $\sim$3 HRI pixels across the minimum dimension; see Klaasen *et al.*, in this issue for a detailed presentation of the expected data from Deep Impact. Earlier images yielded data for navigation and coma science. Use of the filter sets in the day before impact will produce a color lightcurve of the comet as it rotates. These data allow a gross comparison of the side seen at high resolution to the rest of the nucleus. The phase angle increases on approach from 28°, reaching 63° close to impact.

On approach only partial images are taken until 13 min before impact. At this time the nucleus, at 30 m/HRI pixel, is about 200 pixels across, and will present almost as much detail as the recent images of Wild-2. However, beginning at 12 min before impact 7-color data will be taken, providing the first ever high-resolution color stereo coverage of a comet nucleus. Color imaging resumes 240 s after impact when the spacecraft has closed to a pixel scale of 12 m/pixel with the HRI, and continues to a highest color scale of 3 m/pixel; here the nucleus should more than fill the HRI frame.

In the few seconds around impact, imaging by both the MRI and HRI is rapid, partial frames to capture impact phenomena at sub-second intervals. The HRI has a pixel scale of 17 m, the MRI, 85 m, at the predicted impact time, which has an uncertainty of about 6 s, and nominally occurs about 850 s before closest approach. Twenty-four seconds after impact full frames alternate with partial frames, as the range to the comet decreases. The expected $\sim$100 m crater (Schultz and Ernst, this issue) and its ejecta plume will be well characterized by the HRI data. The ITS on the impactor spacecraft will give rapid, partial frames of less than 1 m/pixel just before impact, although cometary dust impacts on the optics may degrade the quality of imaging at some point before impact. Partial frames are used to increase the time sampling available, and still cover virtually the entire visible area of the nucleus with the HRI; ITS partial images close to impact have much smaller fields of view.

The changing geometry during the flyby provides the basis for stereo data, with the usual flyby conditions that while lighting conditions remain essentially fixed, resolution changes. Thus, while the highest resolution HRI images will be about 1.4 m/pixel, stereo convergence angles of $\sim 25^\circ$ are achieved with images of about 3 m/pixel. Four-color stereo of 3 to 6 m/pixel is achieved after impact. Before impact color stereo (7-colors) is achieved between images of about 17 and 30 m/pixel. The highest resolution stereo will include the crater and a significant fraction of the illuminated disk (how much depends on the orientation of the nucleus), the lower resolution stereo will have all the visible disk (less than half the nucleus area). Combination of the ITS images with HRI images provides an additional, higher convergence stereo set, that will at highest resolution cover a small area around the target point (Hampton *et al.*, this issue).

Filters for the MRI (Hampton *et al.*, this issue) are chosen to detect coma components; five of the seven filters in the MRI camera set are narrow bands optimized for coma observations, leaving two wider bands centered at 750 and 850 nm matching those on the HRI. The HRI filters are set at 100 nm intervals between 350 and 950 nm, to determine visible color characteristics without detailed spectroscopy, which investigation is done by the infrared instrument. At visible (.4 to 1 $\mu$m) wavelengths, cometary nuclei exhibit a wide range of linear slopes (Jewitt, 2002). Reasons for this diversity remain unclear.

At scales of meters, we will be able to resolve individual morphologic features and units, which may differ in spectral slope. The HRI filters could detecta change in slope toward the ultra violet as often seen in dark (some C, F- and G-type) asteroids. An increased slope toward the infrared would presumably be due to organics. Silicates, if present, would cause a decrease at near 0.9 $\mu$m. Finally, a neutral slope with high albedo may be indicative of ice. Any variations in color will also be related to the HRI-IR near-infrared spectra, which while at lower resolution, can provide more detailed constraints on composition (see Sunshine *et al.*, this volume). Correlating color variations with specific features and their physical origins may allow us to better understand the significance of slope diversity observed among the comet population. Moreover, Deep Impact's color images will also, provide an opportunity to compare variations observed on the surface, with those exposed in the interior after our impact event.

The near-infrared, long-slit spectrometer has a slit 10 $\mu$rad by 2.5 mrad and spatial pixels of 10 $\mu$rad (assuming $2 \times 2$ binning). It covers the spectral range from 1.05 to 4.8 microns. For details, see Hampton *et al.*, this issue. Spectroscopy on approach is primarily of the coma and is discussed in the article by Sunshine *et al.*, in this issue. The nucleus is an unresolved point source at the center of the slit until well after release of the impactor. Although not spatially resolved, the nucleus will be photometrically resolved at this time, i.e., it will dominate the flux in a single pixel, yielding spectra of the entire illuminated surface as a function of rotational phase. Models of the nucleus, as well as experience with ground-based observations of comets, indicate that the short-wavelength portion of the spectra (1–2.8 $\mu$m)will

be dominated by reflected sunlight while the long-wavelength (2.8–4.8 $\mu$m) portion will be dominated by thermal emission.

After the nucleus becomes spatially resolved, spatial scans are used to map the nucleus with the spectrometer, providing both reflection spectra and thermal emission with varying spatial resolutions. The last pre-impact spectra have a spatial resolution of approximately 100 m on the nucleus; the final spectrum of the impact crater will have a spatial resolution of about 10 m/pixel. With the planned geometry of the encounter, the slit will be oriented parallel to the comet-sun line, with orthogonal spatial scans. Spatial coverage will depend on the orientation of the elongated nucleus, something that can not yet be predicted. The mapping of the reflection spectrum will be used to look for composition variation associated with surface features, while the thermal portion of the spectrum will be used to determine the temperature distribution of the surface layers. Multiple spatial scans will allow a measurement of the phase variation of the spectral reflectance between phase angles of 28–63°.

For later reference we summarize here the best image scales achieved by previous comet flybys. These are about 100 m/pxl for Halley in 1986; 60 m/pxl for Borrelly in 2001; and 15 m/pxl for Wild 2 in 2004. While stereo coverage was obtained both at Borrelly and Wild 2, making it possible to infer surface topography, neither flyby produced high-spatial-resolution color imaging of surface morphology.

## 3. Surface Morphology of Comets

Spacecraft imaging during the past decade has documented a wide variety of processes that determine the evolution of asteroid surfaces. As noted by Malin (1985), comets, thanks to their activity, hold the potential for even greater diversity in terms of surface processes and morphological forms.

Although considerable effort has been devoted to modeling the activity of comets, most such models do not address surface processes in a comprehensive manner, nor make specific predictions of surface morphology. Unfortunately, images of cometary surfaces obtained to date lack the resolution necessary to test such hypotheses in detail. It is noteworthy, however, that the prediction of sublimation producing a "pit and mesa topography" made by Malin and Zimbleman (1986) seems to have been substantiated by the results obtained by Deep Space 1 at Borrelly (Britt *et al.*, 2004) and by Stardust at Wild 2 (Brownlee *et al.*, 2004).

Expectations for the kinds of topographic forms that may occur on the surfaces of comets have concentrated on forms generated by loss of volatiles from within a matrix of silicates, organics, oxides, or other non-volatile materials (Malin, 1985; Colwell *et al*., 1990). The loci, longevity, and strength of active areas of sublimation are expected to change, and this has provided the basis for explanations of changing cometary activity (Sekanina, 1990). The sublimation may be in heterogeneous and

very loose materials, including voids subject to sudden collapse (Whipple, 1950). Internal structures, by providing pathways for evolved gasses, may be important in non-tidal breakups as well as possibly revealing of cometary assembly (Samarasinha, 2001). The great interest in detecting internal structures has to contend with the complexities of the sublimation effects at the surface and their likely overprinting of internal features.

### 3.1. Ablational Features

Ablation of volatile materials and formation of lag deposits should dominate comet nucleus morphology. Only small fractions of nucleus surfaces are active at any one time (Keller, Kramm, and Thomas, 1988; A'Hearn *et al*., 1995); typically over 90% of the nucleus is observed or inferred to be covered with the very dark (albedo $<0.05$) mantling materials. As the surface evolves it is expected that the thickness of the mantling lag deposit will vary across the nucleus. While thick deposits will have an insulating effect, thin layers may enhance sublimation (Malin and Zimbelman, 1986; Colwell *et al.*, 1990).

Sublimation of ices on comets with lag deposits of variable thickness may produce topography analogous to that formed in some terrestrial glacial environments (Malin and Zimbelman, 1986; Colwell *et al.*, 1990). These forms include pit and mesa topography and dust mantled cones and mounds that form by inversion of relief (Malin and Zimbelman, 1986). Dust mantles affect the heating of the volatiles at depth (Brin and Mendis, 1979; Grun *et al*., 1993); they also affect how the gas diffuses to the surface. Porous dust mantles may provide the best insulation, but also may allow the most diffusion of gas from below. It has long been suspected that sections of dust mantles can be blown off, exposing fresh materials and accounting for some cometary outbursts.

Interesting topography may result from inversion of relief and feedback effects on sublimation forms. Inversion of relief occurs when relatively low areas are filled with material that is, or becomes, more resistant to erosional forces than the surrounding materials. On the earth the relevant analogy is covering of snow and ice in low areas by sediment, volcanic ash, or debris flows. The non-volatile covering protects the underlying material from insolation and ablation, and subsequent lowering of surrounding areas yields an inversion of relief: former low areas become relatively high. Inversion can also occur simply due to different amounts of cover. Thin covers can speed up sublimation by lowering the albedo but providing little insulation; thick covers can inhibit sublimation entirely; cover free areas may show an intermediate response (Driedger, 1980; Malin and Zimbelman, 1986).

Feedback effects of topography, most notably focusing of reflected insolation in concavities, can also produce distinctive topography (Colwell *et al*., 1990). Insolation focusing can deepen pits and other depressions, and may even be accompanied by deposition to form a rim. Consistent alignments of conical

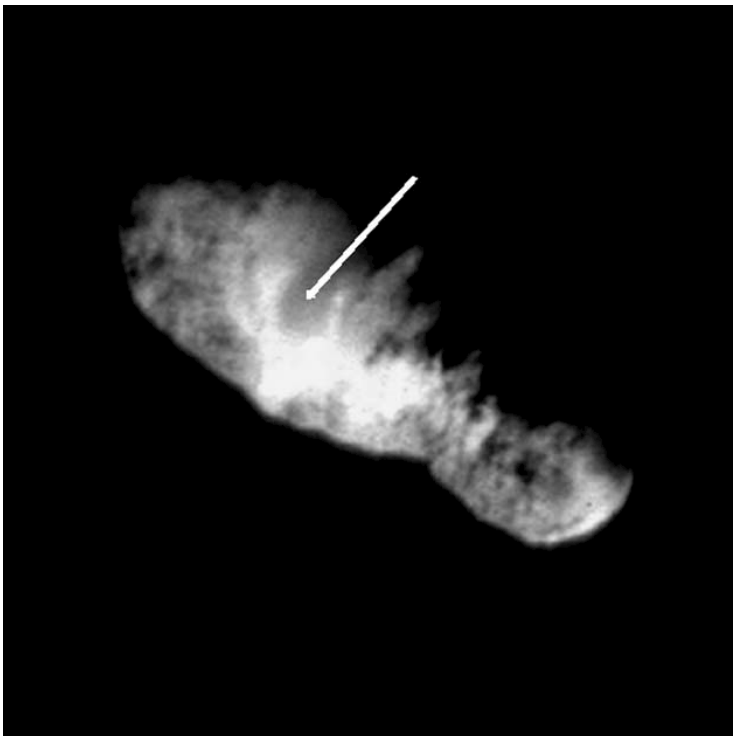

*Figure 1.* Borrelly from Deep Space 1. Nucleus is about 8 km long in this view. Arrow points to middle of largest of the possible mesas.

forms, pits, or asymmetries of mesas or other hills may be useful in limiting the illumination (rotation) conditions under which forms developed, because their formation is a strong function of specific incidence and azimuth angles of insolation.

Images of Borrelly (Figure 1) marginally resolve mesa-like forms (Britt *et al.*, 2004). These may be remnants of a lag deposit formed by backwasting from sublimation of lower, more volatile materials. They could even be examples of inverted relief, where the lag was once in low areas. However, the forms are not sufficiently resolved to allow more than a speculative interpretation.

Images of Wild-2 show many forms that suggest sublimation. (Figure 2). The steep spires, visible on the limb and in stereo, are certainly consistent with, and likely indicative of, sublimation. These reach heights of over 100 m. Brownlee *et al.* (2004) also note the existence of an overhang, almost certainly a form requiring erosional (sublimation in this environment) formation. Much of the topography of Wild-2 seems determined by arcuate ridges and slopes into the depressions,

*Figure 2.* Stereo pair of Wild-2 from Stardust spacecraft. Note the large number of round depressions, many with flat floors, of wide variety of sizes; the arcuate scarps, the pinnacles, and the small patches of relatively high, flat surface. Object is about 5 km across in this view.

strongly indicative of removal of material. More enigmatic is the initiation of the depressions, discussed briefly below.

A major goal of DI high-resolution imaging is to examine ablational landforms in detail and to map their distribution on the nucleus of Tempel 1. We seek to correlate the locations of such features with observed locales of jet activity, with surface expressions of internal structure, and to seek evidence of preferential alignments that might provide clues to past insolation conditions.

### 3.2. REGOLITH

Regolith (loose material of whatever origin) is found on small asteroids, and may exist in some form on comets. Asteroids with surface accelerations in the range of 0.2 to 0.5 cm/s$^2$ easily retain sufficient fractions of crater ejecta to produce morphologically noticeable regolith. An object of dimensions $\sim$2 km, and having a density of about 1 g cm$^{-3}$, has surface gravity $<$0.1 cm/s$^2$, a value not inherently prohibitive of retention of regolith. However, in view of the importance of sublimation and possible compressional influences of cratering in porous targets, regolith on comets may not be developed by the loose particle sedimentation on asteroids and larger rocky objects. Indeed, most speculations about cometary regoliths involve sublimational lag deposits or redeposition of volatiles. A major unresolved question concerns the degree of cohesion of putative cometary regoliths compared to those found on asteroids and the Moon. The mesas on Borrelly suggest some level of cohesion (Soderblom *et al.*, 2004; Britt *et al.*, 2004), and steep slopes and even overhangs on Wild-2 also indicate cohesion (Brownlee *et al.*, 2004).

Although gravity of substantially less than 1 cm $s^{-2}$ is effective at transporting materials across asteroidal surfaces, it is not obvious how well the process will work on rough objects with less than 1/10th as much gravity. Additional complications are that surface topography can change rapidly (geologically speaking) as ablation proceeds. On small satellites and asteroids, downslope motion is most evident where the surface is smoothed by deposition (Thomas *et al.*, 1996), although Eros shows some large, complex slumps (Veverka *et al.*, 2001). The manifestation of downslope motion on comets might be as material ponded in depressions (Robinson *et al.*, 2001), or as streamers down slopes. Detection of material as a separate deposit in the floor of a depression is sometimes difficult. The ponded materials on Eros are easily discriminated because of the high image resolutions, sharp boundaries of the deposits, color variations, and distinctively flat surfaces.

Wild-2 shows flat floors on many depressions, the larger ones of which are attributed by Brownlee *et al.* (2004) to impacts. Color imaging, such as on DI, would be useful in determining if the floors are distinct materials, and if so, might provide evidence for sedimentation, such as in Eros's ponds, or for impact phenomena. Color was used by Robinson *et al.* (2002) to show that the Eros pond material was slightly different from surrounding areas and possibly size sorted from the average Eros regolith.

The much higher resolution of the DI images compared to those obtained by previous missions will make it possible to search for morphological evidence of comet regolith. The data will also be used to map albedo variations across the surface, correlate those with surface morphology, and to delineate the extent of sublimating active areas by high-resolution albedo and morphology information with data on jet location obtained from distant imaging.

Because of the expectation that sublimation plays a dominant role in the evolution of comet surfaces, even though at any one time only a small fraction is "active," a search for asymmetry of features as a function of latitude may prove fruitful. Spin precession may smooth out latitudinal effects; nonetheless, rates may be rapid enough to produce asymmetries of pole- or equator-facing slopes that can be detected by stereoscopic measurements.

### 3.3. Faults, Fractures, Structures

At least three distinct sources of structure can be expected on comet nuclei: those reflecting the initial agglomeration of the paleonucleus, those caused by later impacts and possible reaccumulation of fragments, and those caused by the incompletely understood phenomenon of comet splitting (e.g. Sekanina, 1990). Primary structures resulting from assembly of smaller bodies to form the nucleus (Keller *et al.*, 1986; Weidenschilling, 1997) might comprise variations in porosity, ice/dust ratios, or ice composition. Their visible manifestations might be ridges or troughs that form as a result of spatially varying rates of sublimation. Reassembly structures following

catastrophic breakup would fall in the same category, but being more recent might leave better preserved evidence. Whether the topography associated with such remnants would be prominent enough to be discerned is uncertain. Large, nearly planar features in cometary nuclei might represent metamorphic boundaries (Prialnik and Podolak, 1995) in a larger precursor body, or fracturing in a large body.

Modeling of tidal and other disruptions shows comets can be very weak (Asphaug and Benz, 1994), at least at km scales and probably at 100 m scales (see also the article by Belton *et al*., this issue). Fractures caused by impacts, tidal encounters, thermal changes, or by other stresses may be young relative to the age of the comet or even compared to the time that the comet has been close to the Sun, and thus may be more likely to be detected than formation structures. In certain cases the prominence of fracturing can be enhanced by subsequent sublimation (Colwell *et al.*, 1990). Stereo imaging from DI will permit three-dimensional mapping of prominent structures. Depending on the length or angular extent around the body of a surface linear feature, the feature can be mapped in three dimensions to test whether it may be fracture related (is it somewhat planar?; does it show preferred crossing angles?). The stereo imaging a $>3$ m pixel covering most of the visible disk should allow good characterization of linear features more than a few 100 m in extent. Detection of displacements along fractures would be a major piece of evidence in evaluating comet history and mechanical properties.

The single solar orientation during encounters will require specific care to avoid mapping artifacts of lighting as surface lineations (Howard and Larsen, 1972).

### 3.4. CRATERS

No unambiguous craters are seen in either the Halley or Borrelly images, and there are substantial reasons to question if they are common landforms on comets. The geologically rapid rate of sublimation expected (tens of cm to meters/perihelion passage) is greater than resurfacing rates inferred for Io, which lacks craters of any sort, and may have a crater production rate well above that expected for comets. However, the applicable surface modification rate may be that on the inactive lag areas. Such areas could be modified by slow erosion from diffusing gases or by the fallback of dust ejected at very low speeds. Probably their lifetime is controlled by the migration of centers of activity. The rate of such migration remains poorly known. On Halley, their positions may have remained stable for months (Belton *et al*., 1991), and possible for decades (Schleicher and Bus, 1991). However, even fairly slow migration of small active areas, if changing at a rate of 1 m/perihelion passage, would produce a rapid average turnover compared to average cratering turnover.

Images of Wild-2 by the Stardust spacecraft (Brownlee *et al*., 2004) show nearly circular features, of a wide range of sizes (up to 2 km across), many with flat floors. Bownlee *et al*. attribute those larger than 0.5 km to impact structures, and suggest

that their survival is due to recent perturbation of the comet orbit to the inner solar system. Part of the association with craters was made on the basis of comparison to laboratory impact experiments designed to be scalable to low gravity conditions. If the comparison is valid, the features on Wild-2 have undergone fractionally little degredation, although the spires and other forms on Wild-2 demand substantial erosion, at least 100 m vertically in places, as noted by Brownlee *et al.* (2004). We are of the opinion that an impact origin for the circular depressions observed on Wild 2 remains to be established, and that the smaller depressions are not clearly distinguished from the larger ones on a morphological basis. The basic topography of Wild-2: ridges, pinnacles, and intersecting depressions, may not need impacts for an explanation. The impact experiment on DI will provide an important test by demonstrating the expected morphology of an impact crater on a cometary target.

Craters formed in a thick lag material may have different shapes from those formed through a thin lag into a more porous or volatile substrate. If comet nuclei are low-density porous bodies, the effects of impacts may be different from those on many asteroids or planetary surfaces. Asteroid Mathilde is probably very porous, and displays large craters that leave few signs of damage outside the crater bowl and little evidence of ejecta (Davis, 1999). These craters are likely formed dominantly by compression (Housen, Holsapple, and Voss, 1999), and such might be the norm on cometary nuclei.

The best DI resolution expected, about 1.4 m/pxl from the flyby and 0.5 m/pxl from the impactor, should allow the detection of 5 m craters, and the characterization of 10 m craters, if any exist on the surface of Tempel 1. The recent finding of a deficiency of craters $<$200 m in diameter on asteroid 433 Eros (Chapman *et al.*, 2002) has been explained in two divergent ways. First, that even on small objects, which are not affected by ablation, small craters are erased very efficiently by processes such as seismic shaking induced by impacts (Cheng *et al.*, 2002; Richardson *et al.*, 2004). Second, that our understanding of the population of small impactors far from the Earth-Moon system remains imprecise. The detection of very small craters on the surface of Tempel 1 would serve to constrain the latter possibility. Of course, the spacecraft itself will produce a definitive crater, though we will observe its evolution only for a few minutes.

## 4. Compositional Units

Ground based and spacecraft remote sensing and *in situ* studies have shown that the nuclei of comets contain ices, carbon/hydrogen/oxygen/nitrogen-rich refractory organic solids, and silicate minerals. Many of these materials have characteristic absorption features that are detectable via remote sensing spectroscopic techniques at the near-infrared wavelengths to be measured by the DI spectrometer (Sunshine, this issue). They include rock-forming silicate minerals such as olivine and pyroxene commonly identified in spectra of asteroids and meteorites (e.g., Gaffey

*et al.*, 1989), volatiles like $H_2O$, $CO_2$, CO, HCN, $NH_3$, OCS, $SO_2$, $H_2S$, $CH_3OH$, $CH_4$, $C_2H_2$, $C_2H_6$, and many of the more complex compounds detected in dense molecular clouds. Beyond simple detection of these phases, however, modern radiative transfer and spectral mixture modeling techniques permit quantitative analyses of reflectance and emission spectra for constraining the relative abundances of the components making up the observed surface, and for estimating the dust/ice ratio in different areas.

Recent observations have shown a wide compositional diversity among outer solar system asteroids (Centaurs), planetary satellites, and Kuiper Belt Objects (KBOs). For example, the Centaur object 5145 Pholus shows spectral features indicating the presence of water ice, olivine, and organic molecules–possibly frozen methanol or a photolytic product of methanol (e.g., Cruikshank *et al.*, 1998). On the other hand, Chiron shows a much greyer spectrum dominated by water-ice absorption bands. The DS1 spacecraft acquired a small set of spatially resolved near-IR spectra of parts of the nucleus of Borrelly in the 1.3 to 2.6 $\mu$m region (Soderblom *et al*., 2002). These spectra show a strong thermal emission signature consistent with nucleus surface temperatures in the 300–350 K range. Perhaps not surprisingly (due to these high temperatures), there is no evidence of water or any other ices on the surface of the nucleus. However, there is evidence for at least one spatially varying absorption feature that may be due to the same kinds of relatively simple hydrocarbons inferred for objects like Pholus and some KBOs.

On DI spectral information on scales of 100 m will be correlated with broadband color imaging at 10 m scales to define spectrally distinct units on the nucleus. The composition of the materials in these units, if it can be identified uniquely, will provide important clues to the processes responsible for the formation of the units. Even if such identifications cannot be made uniquely, the patterns observed can provide important clues, for example allowing identification of crater ejecta with a source crater (Geissler *et al*., 1996), or highlighting the presence of layers, or areas of preferred collection of loose materials of distinctive color/spectra.

## 5. Conclusions

Deep Impact data promise to advance our understanding of the processes that control the evolution of comet surface in fundamental ways. First, DI will produce the highest spatial resolution views of any comet surface to date. In addition, it will provide the first high-resolution color imaging in stereo, information which will make it easier to distinguish subtle shading effects due to small scale topography from albedo variations. The extended spectral range of the DI spectrometer enhances the chances of identifying spectrally (and hence, compositionally) distinct units on the nucleus. Finally, thanks to its impact experiments, DI will constrain the currently wide ranging speculations as to what impact craters formed on comet nuclei look like.

## References

A'Hearn, M. F.: 1998, *Ann. Rev. Earth Planet. Sci.* **16**, 273.
A'Hearn, M. F., Millis, R. L., Schleicher, D. G., Osip, D. J., and Birch, P. V.: 1995, *Icarus* **118**, 223.
A'Hearn, M. F., *et al*.: *Space Sci. Rev.* this issue.
Asphaug, E. and Benz, W.: 1994, *Nature* **370**, 120.
Belton, M. J. S.: 2001, *BAAS* **32**, 1062.
Belton, M. J. S., Julian, H. J., Anderson, A. J., and Mueller, B. E. A.: 1991, *Icarus* **93**, 183.
Bleton, M. J., *et al*.: *Space Sci. Rev.* this issue.
Boenhardt, H., Rainer, N., Birkle, K., and Schwehm, G.: 1999, *Astron. Astrophys*. **341**, 912.
Brin, G. D. and Mendis, D. M.: 1979, *Astrophys. J.* **229**, 402.
Britt, D. T., *et al*.: 2004, *Icarus* **167**, 45.
Brownlee, *et al*.: 2004, *Science* **304**, 1764.
Chapman, C. R., Merline, W. J., Thomas, P. C., Joseph, J., Cheng, A. F., and Izenberg, N.: 2002, *Icarus* **155**, 104.
Chapman, C. R., Veverka, J., Belton, M. J. S., Neukum, G., and Morrison, D.: 1996, *Icarus* **120**, 231.
Cheng, A. F., Izenberg, N., Chapman, C. R., and Zuber, M. T.: 2002, *Meteor. Planetary Sci.* **37**, 1095.
Colwell, J. E., Jakosky, B. M., Sandor, B. J., and Stern, A.: 1990, *Icarus* **85**, 205.
Davies, M. E., *et al*.: 1996, *Celest. Mech. Dynam. Astron*. **63**, 127.
Davis, D. R.: 1999, *Icarus* **140**, 49.
Driedger, C. L.: 1980, in Lipman and Mullineaux D. (eds.), *U. S. Geol. Survey Prof. Paper* **1250**, p. 757.
Fanale, F. P., and Salvail, J. R.: 1984, *Icarus* **60**, 476.
Geissler, P., *et al*.: 1996, *Icarus* **120**, 140.
Grun, E., *et al*.: 1993, *J. Geophys. Res*. **98**, 15091.
Hampton, D. L., *et al*.: *Space Sci. Rev.* this issue.
Helfenstein, P. and Shepard, M. K.: 1999, *Icarus* **141**, 107.
Housen, K. R. and Holsapple, K. A.: 1999, *Lunar Planet. Sci*. **30**, Abstract 1228.
Housen, K. R., Holsapple, K. A., and Voss, M. E.: 1999, *Nature* **402**, 155.
Howard, K. A. and Larsen, B. R.: 1972, *Apollo 15 Preliminary Science Report*, 25–58 to 25–62, NASA, Washington DC.
Jewitt, D.: 2002, *In Proceedings of Asteroids, Comets, and Meteors, 2002*, Abstract [01-00i].
Keller, H. U., *et al*.: 1986, *Nature* **321**, 320.
Keller, H. U., Kramm, R., and Thomas, N.: 1988, *Nature* **331**, 227.
Klaasen, K. P., *et al*.: *Space Sci. Rev.* this issue.
Malin, M. C.: 1985, in *NASA Tech, Mem.* 87563, p. 83.
Malin, M. C. and Zimbelman, J. R.: 1986, *Lunar Planet. Sci. Conf.* **17**, 512.
Meech, K. J., Fernandez, Y., and Pittichova, J.: 2001, *Bull. Am. Astron. Soc.* **33**, 1075.
Miller, J. K., *et al*.: 2002, *Icarus* **155**, 3.
Prialnik, D. and Podolak, M.: 1995, *Icarus* **117**, 420.
Prockter, L. M., Thomas, P. C., Robinson, M., Joseph, J., Milne, A., Bussey, B., *et al*.: 2002, *Icarus* **155**, 75.
Reitsema, H. J., Delamere, W. A., and Whipple, F. L.: 1989, *Science* **243**, 198.
Richardson, J. E., Melosh, H. J., and Greenberg, R.: 2004, *Lunar Planet. Sci. Conf.* **35**, abstract 1864.
Samarasinha, N.: 2001, *Icarus* **154**, 540.
Schleicher, D. G., Bus, S. J.: 1991. *Ast. J.* **101**, 706.
Schultz, P. H. and Ernst, C.: *Space Sci. Rev.* this issue.
Sekanina, Z.: 1990, *Ast. Jour.* **100**, 1293.
Soderblom, L., *et al*.: 2002, *Lunar and Planetary Science Conference* **33**, March 11–15, 2002, Houston, Texas, Abstract no.1256.

Soderblom, L. A., *et al*.: 2004, *Icarus* **167**, 4.
Sunshine, J. M., *et al*.: *Space Sci. Rev.* this issue.
Thomas, P. C., *et al*..: 2002, *Icarus* **155**, 18.
Thomas, P. C., *et al*.: 1994, *Icarus* **107**, 23.
Thomas, P. C., *et al*.: 1996, *Icarus* **120**, 20.
Veverka, J., *et al*.: 2001, *Science* **292**, 484.
Weidenschilling, S. J.: 1994, *Nature* **368**, 721.
Weidenschilling, S. J.: 1997, *Icarus* **127**, 290.
Whipple, F.: 1950, *Astrophys. J.* **111**, 375.